

2018



**25th Congress of
International Federation for
Heat Treatment and Surface Engineering**

11-14 September 2018 | Xi'an China

PROCEEDINGS



Organized by Chinese Heat Treatment Society (CHTS)

25th IFHTSE CONGRESS PROCEEDINGS

11-14 September 2018

Xi'an China



Chinese Heat Treatment Society

Tel: +86 (0) 10 6292 0613 • Email: chts@chts.org.cn • Web: www.chts.org.cn

Add: 18 Xueqing Rd., Beijing, China

Microstructure and mechanical properties of SA336F12 fabricated by electricity melting additive manufacturing technology.....	275
Mechanical properties and corrosion behaviors of TiN/TiAlN multilayer coatings by ion source enhanced hybrid arc ion plating.....	276
The methodology research of industrial design for remanufacture.....	276
Microstructure and tensile properties of laser additive repaired titanium alloy.....	277
Effect of annealing on the microstructure properties of supersaturated Cu-Cr alloy film and bulk.....	277
High temperature oxidation behaviors of HVOF-sprayed Cr ₂ C ₃ -NiCr coating in air at 800 °C.....	278
Grain morphology evolution and texture characterization of wire and arc additive manufactured Ti-6Al-4V.....	278
The thermal fatigue behavior and cracking characteristics of ductile Ni-resist cast iron for exhaust manifolds.....	279
Influence of Al content on microstructure and properties of TC4 alloys fabricated by laser additive manufacturing.....	279
Microstructure and electrochemical anodic behavior of Inconel 718 fabricated by high-power laser solid forming.....	280
A constitutive model for high temperature deformation of AZ31 magnesium alloy.....	280
Microstructure and wear resistance of in-situ synthesized (Ti ₃ Al+TiB)/Ti composites by laser surface additive manufacturing.....	281
Localized grain boundary melting induced HAZ liquation cracking during laser solid forming of IN-738LC superalloy.....	281
The effect of micro-B addition on microstructure and mechanical properties of laser additive manufacturing Ti-6Al-4V.....	282
Mechanical properties and microstructural characterization of bronze fabricated by selective laser melting.....	282

New Technologies for Hard and Superhard Thin Films

Plasma surface niobium alloying on pure titanium surface.....	283
Simulation of residual stress of different TiN coating systems on Be substrate.....	284
Tuning the growth and surface enhanced Raman effect of graphene layers for adsorbed single molecules.....	285
Plasma spraying process and corrosion resistance of NdFeB alloy surface.....	286
Comparison in wear properties and cutting performance of TiAlN and TiAlN/MoN multilayer coatings deposited by magnetron sputtering.....	287
The growth of TiCN films by arc ion plating.....	288
Structural evolution and properties of hydrogenated W-doped DLC films.....	289
Influence of nitrogen implantation on optical properties of CVD bulk diamond and diamond films.....	292

Effect of graphene oxide additive on tribocorrosion behavior of MAO coatings prepared on Ti6Al4V alloy.....	293
Study on energy resolution of high quality single crystal diamond α particle detector.....	293
Effect of micro-arc oxidation electrolyte and voltage on growth of LDHs film.....	294
Superhard nanocomposite films deposited by filtered cathodic vacuum arc.....	294
Ultra-smooth and hydrophobic ultra-nano-crystalline diamond film growth in C-H-O-N gas phase system via microwave plasma CVD.....	295
Structure and tribocorrosion properties of coupled coatings of TiSiCN/nitride on Ti6Al4V alloy.....	295
Excellent adhered thick diamond-like carbon coatings by optimizing hetero-interfaces with sequential highly energetic Cr and C ion treatment.....	296
Element diffusion and self-healing performance of MoSiAlY coating on γ -TiAl substrate by a surface alloying method at 900 °C.....	296
The behavior of Ag in TiSiN coating and the properties of the composite coating.....	297
Tribological behavior of epoxy coatings modified by nano filler ($Al_2O_3/WC-Co$).....	297
Study on the modification of high energy titanium ion implantation on the surface of aluminum alloy.....	298
Si-DLC films with excellent tribomechanical properties.....	298
Abrasion and erosion behavior of DLC-coated oil-well tubing in a heavy oil/sand environment.....	299
Synthesis of monolayer MoN and nanomultilayer MoN/CrN coatings using cathode arc plasma vapor deposition.....	299
Effect of cathode arc current on the oxidation and seawater corrosion resistance properties of Cr-Si-N coatings deposited by cathode rotating arc ion plating.....	300
Hard and highly adhered a-C:H gradient coating fabricated by stress editing.....	300
Effects of Ta, W doping on O adsorption and oxidation at the γ TiAl (111) surface.....	301
Surface functionalized diamond for advanced engineering application.....	301
Analysis of residual stress and interface bonding strength of TiN coating.....	302
Effect of programmable ion permeation (PIP) technology on microstructure and corrosion resistance of 304 stainless steel.....	302

High-power Impulse Magnetron Sputtering, HiPIMS

Plasma diagnostics in HiPIMS.....	303
Effects of HiPIMS pulse-length on plasma discharge and on the properties of WC-DLC coatings.....	304
High power impulse magnetron sputtering based on novel waveform configuration.....	305
Discharge characteristics of superimposed HiPIMS-MF and properties of as-prepared nitride nanocomposite coatings.....	305

Plasma surface niobium alloying on pure titanium surface

Wenbo Wang

(School of mechanics, Taiyuan University of Technology)

wwb65@163.com

Abstract: Ti-45Nb is a typical Ti-Nb alloy which possesses burn-resistant property as well as superior corrosion resistance and mechanical properties. However, high content of expensive niobium makes the production of this alloy very costly and also reduces the specific strength. In this study, a Ti-Nb alloyed layer is prepared on surface of pure titanium by double glow plasma surface alloying process. Because niobium has the lowest heat of oxidation (on a mass basis) among metals showing extensive solubility in titanium, researchers reasoned that it should be the most effective element for reducing combustibility. It is anticipated that so long as the surface alloying layer could obtain the required Nb composition and enough thickness, it would present the characteristics of the Ti-45Nb alloy. In this way, these conventional titanium alloys are endowed with the properties of Ti-Nb alloy cost-effectively and the high specific strength of the bulk material is remained.

The process is carried out in a vacuum glow discharge sputtering chamber in which a pure niobium plate is used as the sputtering target and substrate materials are the titanium alloys to be treated. Pure argon is used as discharge media. Glow discharges are ignited on the target and substrate separately with two sets of DC power suppliers and heat them to high temperature. Niobium particles are sputtered out from the target and deposit on surface of substrate. The alloyed layer is formed thereafter through diffusion process producing strong metallurgical bonding with the substrate. Major parameters involved in this process are processing temperature, holding time, sputtering voltage, substrate voltage, working pressure, distance between the target and substrate. In order to obtain the high quality alloying layer with desired content and effective thickness a large number of experiments should be performed to optimum process parameters. Moreover, cleanliness of the substrate surface also affects the formation and growth of the alloyed layer significantly. It is necessary to clean the substrate with argon sputtering prior to the diffusion process. Experiments show that the voltage difference between the target and substrate is a very important factor to control the quality of the alloyed layer. The compositions of the alloyed layers are analyzed by glow discharge spectrum analyzer (GDA). The results show that alloyed layer with surface niobium content close to Ti-45Nb is obtained and the niobium content decreases gradually from surface to substrate. Microstructure and hardness of the alloyed layers are also analyzed by optical microscope and Vickers hardness tester, X-ray diffraction and scanning electron microscope respectively. The combination of SEM and XRD is used to investigate morphology and structure of the surface alloying layer.

It could be concluded that plasma surface niobium alloying on pure titanium is a practicing method for improving the properties of pure titanium, thus increasing the field of application of titanium and its alloys. Adjusting the processing parameters properly, thickness and surface composition of the alloyed layer could be controlled. The microstructure, chemical composition and hardness of the surface alloying layers were analyzed to understand the mechanisms of surface alloying. These results can be explained according to the diffusion theory.

Keywords: plasma surface alloying, pure titanium, niobium, microstructure

Simulation of residual stress of different TiN coating systems on Be substrate

Chengming Li, Liangxian Chen, Lihuan Wang
(University of Science and Technology Beijing, China)
wlh9508@126.com

Abstract: In this paper, based on the Ti-based PVD coating, the optimization of the design of the wear-resistant system of the hemispherical dynamic pressure motor is studied. For the different properties of Be, Ti and TiN, like conductivity, density, elastic, expansion and specific heat, Abaqus finite element numerical calculation was used to simulate the single-layer TiN coating on Be substrate, TiN coating with the Ti transition layer, gradient coating and graded coating, and analyze the residual stress distribution status of the coating under different conditions. The results show that the changed trend of residual thermal stress on the TiN coating is consistent when the coating structure is changed in the same way in different models. Only increase the coating thickness from 5 μm to 30 μm , the residual Mises stress of TiN coating increases about 5%. Under the same total coating thickness 30 μm , as the thickness of the transition layer increases from 1 μm to 9 μm , the residual Mises stress of TiN coating decreases from 1810 MPa to 1475 MPa. Keeping same total coating thickness and increasing the number of coatings in the graded coating structure can't effectively reduce residual thermal stress. When the properties of the transition layer gradually convert from Ti to TiN, the residual thermal stress on the TiN coating is the smallest. This result has guiding significance for the optimal design of hard coatings.

Keywords: coating, stress analysis, simulation

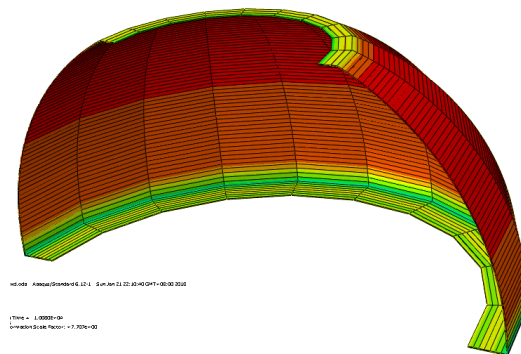


Fig.1 Distribution of Mises stress on the TiN coating of 30 μm thickness

Tuning the growth and surface enhanced Raman effect of graphene layers for adsorbed single molecules

Xiaying Li, Shiping Zhang, Jiakai Nie, Changmin Xiong, Ruifen Dou
(Department of Physics, Beijing Normal University)
rfdou@bnu.edu.cn

Abstract: Graphene, a single sheet from graphite, has the ideal 2D structure with a monolayer of carbon atoms packed into a honeycomb crystal plane^{1, 2}. The 2D layered graphene has been a promising candidate for electronic applications due to its high mobility, and its chemical and mechanical stability. Besides, due to its biocompatible, graphene has potential bioapplications. Very recently, it is reported that graphene can be a suitable substrate for surface Raman enhancement study of adsorbed molecules^{3, 4}. Surface-enhanced Raman spectroscopy (SERS) is a powerful approach to characterize structures of chemicals at extremely low concentrations or even at the single molecule level. In this contribution, we have synthesized the graphene layers with large-size and high quality on copper foil and SiO₂/Si surfaces by using chemical vapor deposition (CVD) through optimizing the growth parameters. Meanwhile, we further robustly transfer graphene layers onto Ag substrate for comparing the substrate effects on the SERS. After respective deposition of low-coverage of Mn12 single molecule magnets onto Graphene/Cu, Graphene/SiO₂/Si and Graphene/Ag (Mn12-1LG-SERS) surface, we find that the Raman scattering signals of single molecules of Mn12-ac on monolayer Graphene/Ag surface are obviously enhanced compared that on the Cu surface and SiO₂/Si surface. The enhancement mechanism of SERS for the Graphene/Ag system can be understood based on the cooperative effect both of Ag nano particles (NPS) and the weak interaction between Ag and graphene monolayer. Ag NPS are spontaneously generated by annealing the Graphene/Ag sample when transferring the graphene layer onto the Ag substrate. Ag NPS can induce the local surface plasmon resonance and formation of a strong localized electromagnetic field between graphene and metal foil, which is called as the EM effect. Also, the weak interaction between graphene and Ag NPs results in the localized surface plasmon resonance can be brought out and enhanced once more. The cooperation of above two effects makes the graphene monolayer/Ag NPs system as an optimal surface for enhancement of Raman spectroscopy. We expect that this system also can be used to realize the SERS when detecting other molecules even though the molecular coverage is reduced to single molecule.

Keywords: graphene, single molecule magnet (Mn12-ac), support substrates (Ag, Cu and SiO₂/Si), surface enhance Raman spectroscopy (SERS), nano particles

Plasma spraying process and corrosion resistance of NdFeB alloy surface

Cheng Gao¹, Yuqi Zhao², Dayong Cai¹, Jinyong Xu², Qin hao Zhao²

(1. School of Materials Science and Engineering, Yanshan University;

2. School of Mechanical and Electrical Engineering, Guilin University of Electronic Technology)

Abstract: NdFeB permanent magnet has excellent magnetic properties and mechanical processing characteristics, but their rich in element lanthanum, the chemical properties are lively, and NdFeB permanent magnet alloys are generally prepared by the sintering process, there are a large number of micro-holes on the surface, microscopic loose structure. This makes the NdFeB permanent magnet alloy vulnerable to corrosion damage caused by the galvanic effect in a hot and humid environment. Using plasma spray technology to protect the surface of NdFeB permanent magnet alloy, Al₂O₃ ceramic layer was prepared to improve its corrosion resistance. In this study, the spraying voltage, the spraying current, the main gas flow rate and the spraying distance in the plasma spraying process were selected as the factor variables of the process parameters, and the orthogonal test optimization was performed. The test includes the determination and analysis of the average micro-hardness of the ceramic layer of the sample, the determination and analysis of the bonding strength of the ceramic layer, the observation of the surface and cross-sectional morphology of the ceramic layer and the X-ray diffraction pattern analysis, the assessment of the macroscopic appearance of the salt spray corrosion of the ceramic layer, and ceramics. The corrosion rate of the layer in a 3.5wt% NaCl solution was determined and analyzed. The results show that there are three main phases in the ceramic layer, namely the mutual dissolution zone of Al₂O₃ and TiO₂ in the gray band, i.e, the Al₂TiO₅-enriched zone, the TiO₂-enriched zone in the light white zone, and the Al₂O₃-enriched zone in the gray-black zone. The TiO₂ and the Al₂O₃-enriched parts are mutually melted, so that the internal polymerization strength of the ceramic layer is improved. The doping of TiO₂ well inhibits the nucleation rate of γ -Al₂O₃ during the spraying process, delays the transformation process of α -Al₂O₃ to γ -Al₂O₃ phase, refines the grain and presents an amorphous structure, and the hardness of the ceramic layer. And significantly improved corrosion resistance. The average micro-hardness exceeds 790 HV0.3, up to 900 HV0.3. The sample was continuously sprayed with (3.5±0.2)wt% NaCl solution, and the macroscopic morphology of the ceramic layer after 250 h was graded according to the percentage of surface defects, and the best ceramic layer quality was 0 grade, indicating that the coating has excellent corrosion resistance. The best set of samples had a corrosion potential of -380 mV and a corrosion current of 0.0010 mA/cm². The single phase of γ -Al₂O₃ contained in the ceramic layer reacts with H⁺ and (OH)⁻ to form free Al³⁺ and (AlO₂)⁻. The reason for the different rate of corrosion weight loss is that Al₂O₃ and (OH)⁻ react to Al(OH)₃ colloids, in turn, continue to react to form free (AlO₂)⁻, which have a deterrent effect on the rate of corrosion weight loss. Orthogonal experiments show that the primary and secondary influence law of the process factors on the corrosion resistance of the ceramic layer is A (spray voltage)> D (spray distance)> C (main air flow)> B (spray current), and the intensity ratio is about 4:1.25:1:1. The best spraying process parameters for the corrosion resistance of the ceramic layer in the horizontal range of the selected factor are: spraying voltage 48 V, spraying current 450 A, main gas flow 2300 L/h, spraying distance 115 mm.

Keywords: plasma spraying technology, ceramic layer, corrosion resistance

Comparison in wear properties and cutting performance of TiAlN and TiAlN/MoN multilayer coatings deposited by magnetron sputtering

Tao Wang¹, Li Wang¹, Yan Li², Guojun Zhang¹

(1. School of Materials Science and Engineering/Xi'an University of Technology;

2. School of Mechanical and Precision Instrument Engineering/Xi'an University of Technology)

twang@xaut.edu.cn, zhangguojun@xaut.edu.cn

Abstract: TiAlN coating has been widely used as wear-resistant hard coating on cutting tools in the past decades for its high hardness and oxidation resistance. Nowadays, as green manufacturing become the main trend of machine building industry, the hard coatings used on cutting tools should not only have higher hardness and better oxidation resistance but also lower coefficient of friction (COF). Since TiAlN coating generally exhibits a high COF, lots of efforts have been made on decreasing the COF of TiAlN coating by incorporating V, Mo, W elements, which can generate lubricious Magnesium oxide phase during friction. However, the cutting performance of these coatings has not been investigated yet. Therefore, in this paper, a comparison in cutting performance of TiAlN and TiAlN/MoN multilayer coating was made. The TiAlN and TiAlN/MoN multilayer coating were deposited on silicon wafers, high speed steel (HSS) plates and high speed steel drills. The microstructure, mechanical and wear properties was characterized by TEM, SEM, nano-indentation, Rockwell C indentation and ball on disc test. The cutting performance of uncoated, TiAlN and TiAlN/MoN coated drills was evaluated by drilling test on thick 1045 carbon steel plate. It was found that both of TiAlN and TiAlN/MoN multilayers coatings exhibit a face center cubic structure similar to B1-NaCl. The modulation period of TiAlN/MoN multilayers was 8.6 nm and the modulation ratio was 1:2 (TiAlN: MoN). The TiAlN/MoN multilayers coating exhibit a higher hardness (31.1 GPa) than that of TiAlN coating (24.7 GPa). The COF of TiAlN/MoN multilayer coating was only one half of that of TiAlN coating. After sliding against WC ball for 850 m, the TiAlN coating was completely worn out while TiAlN/MoN multilayer coating exhibited a low wear rate of $8 \times 10^{-17} \text{ m}^3/(\text{N}\cdot\text{m})$. In case of dry cuttings, both of TiAlN and TiAlN/MoN multilayer coated drills exhibited much better cutting performance compared to the uncoated HSS drills. The flank wear of TiAlN/MoN coated drill was 40%-50% of that of TiAlN coated drills after drilling the same numbers of holes, suggesting an improvement in cutting performance of TiAlN/MoN multilayer coating compared to TiAlN coating.

Keywords: hard coating, TiAlN, TiAlN/MoN, cutting performance

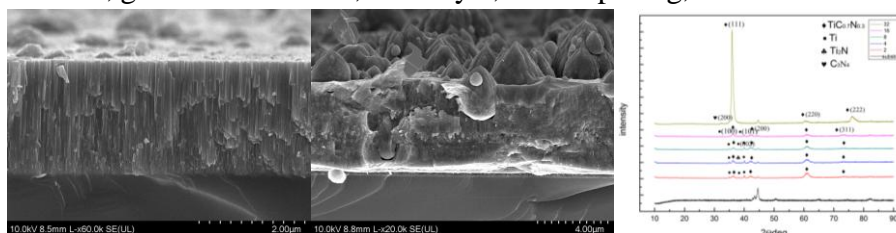
The growth of TiCN films by arc ion plating

Lian Liu, Qian Shi, Mingjiang Dai, Songsheng Lin, Hong Li, Chaoqian Guo
(Guangdong Institute of New Materials)
459219887@qq.com

Abstract: TiCN coating possesses excellent wear resistance, anti-corrosion and high hardness, thus it has been widely used as an engineering ceramic, such as cutting and medical tools. TiCN is a solid solution of TiN and TiC and would incorporate the advantages and characteristics of both. However, seldom researches have involved in the grains growth mechanism of TiCN films. Unlike bulk materials, which growth of grain just involves interfacial free energy, the grain growth in the films is generally more complicated. For thin films, the free energy associated with the substrate and film interface play an important role in grain growth. For thinner films, it has been reported that the effect of abnormal crystal grain growth is more pronounced. In order to obtain different grain growth patterns, we designed monolayer and multilayer TiCN films with the same deposition time. In this study, TiCN films with different modulation period and monolayer TiCN films were deposited under same process parameters by arc ion plating technology. The cycle number of the multilayer film is 2, 4, 8, 16, and 32 respectively. It is obvious that the grain boundary can promote the continuous precipitation of the solutes when crystal grain is supersaturated. In this process, the energy is mainly controlled by the solute morphology and the entropy change. So we put as much CH₄ gases as possible into the arc ion plating equipment to ensure the carbon is supersaturated in TiCN films. And the growth mechanism was studied. Surface and cross-section morphology, phase structure and composition of the films were analyzed by scanning electron microscopy (SEM), X-ray diffraction (XRD) and energy dispersive spectrometer (EDS). The hardness of the films was performed by micro Vickers-hardness tester, and the thickness was examined by 3D profiler, and the scarification test was carried by multifunctional material surface tester.

The results showed that we obtained different grain patterns of TiCN films by controlling the modulation period. From XRD and cross-section topography results, monolayer film and multilayer films with 32 cycles had a strong (111) preferred orientation with columnar crystals of growth. However, the multilayer films with 2 to 16 cycles changed in the growth orientation from (111) to (220) preferred orientation. And the cross section penetrates the large droplet-like tissue. The EDS results showed that the elements content of droplet-like tissue was similar with the films, and the hardness is over 3200 HV. This indicated that the droplet-like tissue is another form of TiCN instead of titanium metal droplet. What's more, the carbon content of the droplet-like tissue was higher than the carbon content of TiCN films. It is indicated that the interface precipitates carbon and promotes abnormal grain growth. In these TiCN films, we detected that there are three forms of carbon including free carbon, solid solution carbon and CN_x. And the hardness, texture and the grain growth mechanism of these films were strongly effect by thickness of each layer. With the increase of cycles, the thickness of each layer in this film reduced and the formation of carbon and the microstructure of TiCN changed. It is indicates that the forms of carbide in TiCN films can be controlled by carbon content and modulation period, which therefore provides reference to obtain TiCN films with excellent mechanical properties.

Keywords: TiCN films, growth mechanism, multilayer, arc ion plating, microstructure



Structural evolution and properties of hydrogenated W-doped DLC films

Wei Xu^{1,2}, KeSong Zhou^{1,2}, Songsheng Lin², Mingjiang Dai², Chunbei Wei², Qian Shi²

(1. School of Material and Engineering, Central South University, Changsha, China;

2. Guangdong Institute of New Materials, National Engineering Laboratory for Modern Materials Surface Engineering Technology, The Key Lab of Guangdong for Modern Surface Engineering, Guangzhou, China)

xuw0907@163.com

Abstract: Diamond-like carbon (DLC) films have found a wide range of industrial applications including bearings, drills, molds, artificial prosthetics and magnetic recording devices, owing to their unique combination of superior properties, such as high hardness, low friction coefficient, good wear resistance, biocompatibility and chemical inertness. Unfortunately, the main drawbacks of DLC films like high internal stress ranging from several gigapascals to 10 GPa and poor adhesion to the underlying substrates may cause a premature failure and delamination, drastically limiting their practical applications. In order to overcome the drawbacks of DLC without losing the beneficial properties of the pure films, hydrogenated W-doped diamond-like carbon films were prepared by a hybrid plasma deposition approach combines magnetron sputtering and anode layer ion source, which allows independent control of the incorporated-W content and carbon film structure. The micro morphology and structural evolution of the films were investigated by using atomic force microscope (AFM), scanning electron microscope (SEM), high-resolution transmission electron microscope (HRTEM), X-ray diffraction (XRD) and Raman spectroscopy. The mechanical properties of the films were determined by nano-indenter and residual stress tester. The results show that the surface morphology of as-deposited films evolved from an ultra-smooth surface to a rough surface with a large amount of spherical nano-particulates with the increasing of tungsten target current. A typical nanocomposite structure was mainly formed at the low target current of 1 A, with the target current increasing, it transforms to a nanolayered superlattice structure where the layers are periodically repeated with individual thickness less than 10 nm. It was found that the amount percent of sp^2 hybridization carbon atoms determined by the electron energy loss spectroscopy (EELS) increases from 60.4% to 82.1% with the increasing of target current from 1 A to 3 A. A significant residual stress reduction was found in W-doped DLC film compared with pure one (3.8 GPa). The hardness and elastic modulus of the films increase monotonously with the target current increasing. Comparing the tribological properties of the films with nanolayered structure, the film with more homogeneous dispersion of WC_{1-x} nanocrystallites throughout the carbon-based matrix exhibits better in anti-friction and wear resistance. These results indicate that it is possible to prepare Me-doped DLC films with tailored microstructure and desirable properties for specific applications.

Keywords: diamond-like carbon, W-doped, structure, EELS, nanocomposite, nanolayered

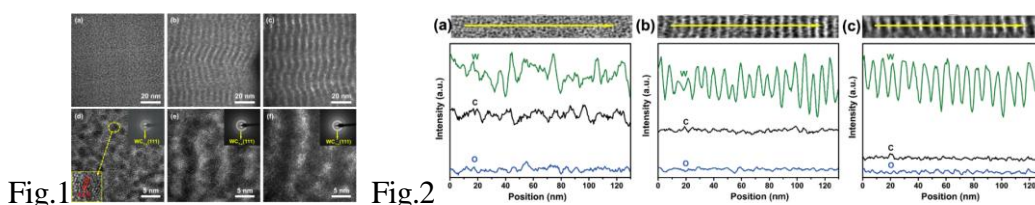


Fig.1 High-resolution TEM images and corresponding SAED patterns:(a, d)1 A; (b, e)2 A; (c, f)3 A

Fig.2 High-resolution TEM images and corresponding EDS line scanning patterns:(a)1 A; (b)2 A; (c)3 A

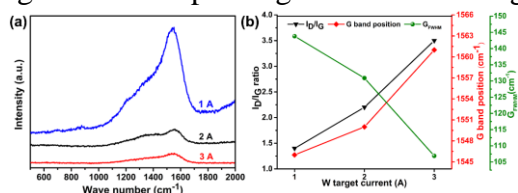


Fig.3 (a)patterns of W-DLC films deposited at different tungsten target currents and (b) fitted results

Improved oxidation of CoNiCrAlTaHfY coatings on C/C composites by adding Co intermediate buffer layer

Q. Guo, T. X. Meng, W. Q. Ding, W. Xi, H. G. Yan, N. M. Lin, S. W. Yu, X. P. Liu

(Research Institute of Surface Engineering, Taiyuan University of Technology, Taiyuan 030024, China)

liuxiaoping@tyut.edu.cn

Abstract: C/C composites are one of the most potential materials in aerospace and auto industries due to their excellent properties, but they are used sparingly at the elevated temperature due to the poor oxidation in the air when the temperature is above 370 °C. For example, 1% of weight loss caused by oxidation could lead to 10% reduction in strength of C/C composites. MCrAlY (M=Co,Ni) alloy as a common material of thermal barrier coatings is related its good high-temperature resistance. In the paper, the CoNiCrAlTaHfY/Co composite coating in C/C composite surface was prepared by using plasma surface alloying to improve their oxidation behavior.

The CoNiCrAlTaHfY/Co composite coating was prepared in C/C composite surface by duplex plasma alloying of Co single-element (850 °C/1.5 h) and Co-Ni-Cr-Al-Ta-Hf-Y multi-element penetrations (900 °C/3 h). The C/C composite was etched firstly by H₂+Ar (850 °C/2 h) using microwave plasma chemical vapor deposition prior to Co-alloying to activate the C/C composite surface. Microstructure and composition of alloyed C/C composites were analyzed by scanning electron microscopy (SEM), energy dispersive spectroscopy (EDS) and X-ray diffraction (XRD). The oxidation experiment of as-prepared coatings was carried out in air at 1000 °C and the oxidation behavior was evaluated by weight loss rate.

Fig.1 shows the surface morphology of bulk C/C composites and after H₂+Ar etching at 850 °C for 2 h. The carbon fibers in the unetched surface were tightly surrounded by continuous carbon matrix (Fig.1a), and after plasma etching, they became cone-shaped fibers in the thin-walled carbon tubes.

Fig.2 shows the surface and cross section of CoNiCrAlTaHfY coating on C/C composite surface without and with etching. About 10 μm-thick coating on unetched surface with some cracks separated from substrate (Fig.2a). The thickness of the CoNiCrAlTaHfY coating on the etched substrate was about 14 μm and the bonding strength between coating and substrate was improved though still with a few penetrating cracks (Fig.2b).

Fig.3 shows the cross sectional morphology and composition of CoNiCrAlTaHfY/Co composite coatings formed on etched C/C composites. The movement of alloying elements of Co, Ni, Cr, Al, Ta, Hf, Y into the Co buffer layer and Co atoms in the buffer layer into substrate led to a homogeneous composite coating adhered to substrate. The CoNiCrAlTaHfY/Co coating with 16 μm-thick CoNiCrAlTaHfY top layer and 8 μm-thick Co transition layer was composed of CrCoTa, Al₂Ta, Cr₂Ta, Al_xCr_y, AlCo₂Ta, Co and Al_xNi_y.

Fig.4 shows the weight loss of bulk C/C composites and CoNiCrAlTaHfY/Co composite coatings after exposure in air at 1000 °C. The C/C composite was 56.8% in weight loss after 120 min oxidation and volatilized totally in 240 min. The CoNiCrAlTaHfY/Co composite coating presented an improved oxidation resistance due to their lower weight loss. From the surface morphology and XRD pattern of the oxidized composite coating shown in Fig.5, the oxidized surface was compact and mainly covered by the Cr₂O₃+Al₂O₃ mixed oxide.

The CoNiCrAlTaHfY/Co composite coating with 25 μm in thickness was formed on etched C/C composites. The compact composite coating was composed of CrCoTa, Al₂Ta, Cr₂Ta, Al_xCr_y, AlCo₂Ta, Co and Al_xNi_y. The mutual diffusion among the CoNiCrAlTaHfY top layer/Co transition layer/substrate resulted in a strong adhesion between coating and substrate. After exposing in air at 1000 °C for 4 h, the bulk C/C composite volatilized completely, while the loss rate of CoNiCrAlTaHfY/Co composite coating was about 0.82%, showing an improved oxidation resistance.

Keywords: C/C composite, MCrAlY multi-alloying, Co-buffer layer, high-temperature oxidation

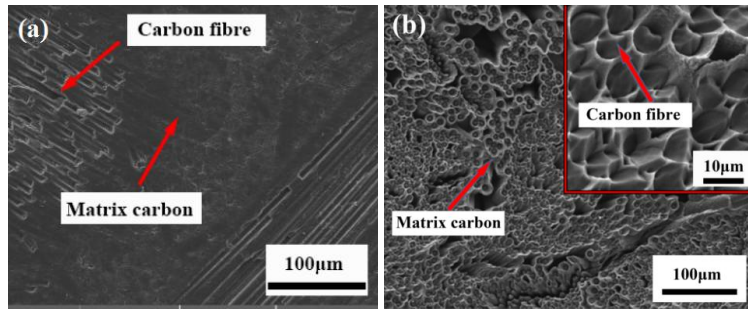


Fig.1 Surface morphology of (a) unetched and (b) etched C/C composites

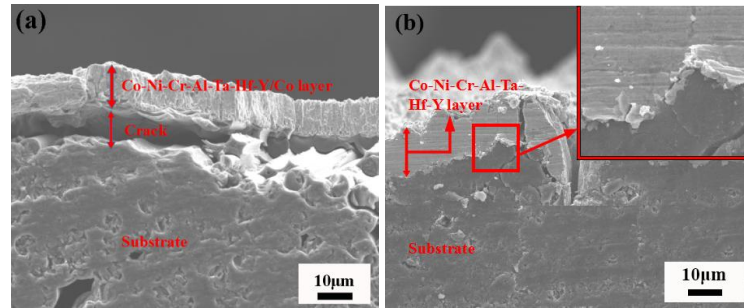


Fig.2 Cross section of CoNiCrAlTaHfY coatings on (a) unetched and (b) etched C/C composites

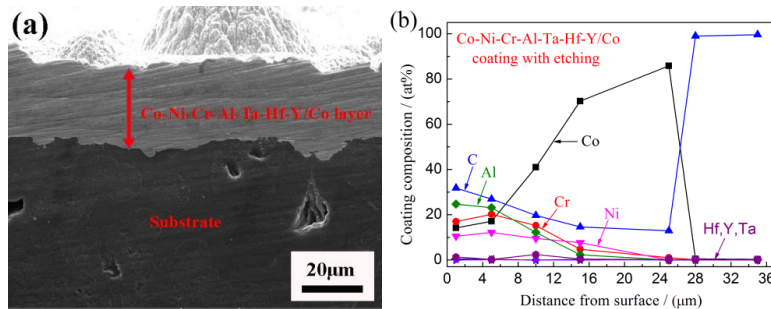


Fig.3 Cross sectional morphology and composition of CoNiCrAlTaHfY/Co coatings

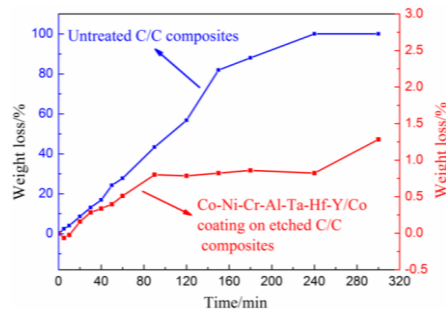


Fig.4 Weight change of bulk C/C composites and CoNiCrAlTaHfY/Co coatings

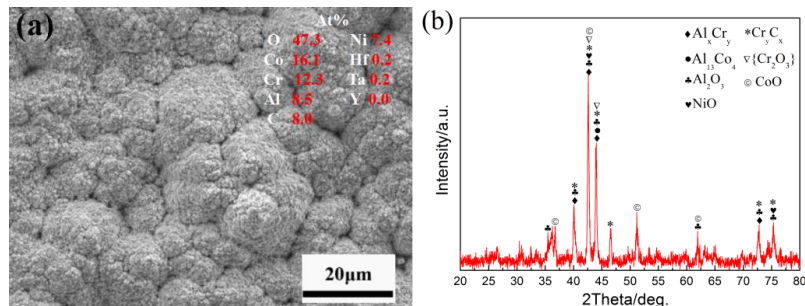


Fig.5 Surface morphology and XRD pattern of CoNiCrAlTaHfY/Co coatings

Influence of nitrogen implantation on optical properties of

CVD bulk diamond and diamond films

Tomasz J. Ochalski^{1,2}, Haitao Ye³, Dzianis Saladukha^{1,2}, Sini Nanadath Shibu^{1,2}, Junjun Wei⁴,
Kang An⁴, Chengming Li⁴

(1. Department of Applied Physics and Instrumentation, Cork Institute of Technology, Rosa Avenue, Cork T12 P928, Ireland; 2. Tyndall National Institute, University College Cork, Cork T12 R5CP, Ireland; 3. University of Leicester, University Road, Leicester LE1 7RH, UK; 4. Institute for Advanced Materials and Technology, University of Science and Technology Beijing, Beijing, China)

Abstract: In order to enhance fluorescence intensity we propose ion implantation followed by diamond irradiation by high energy particles or radiation, usually at energy of 30 keV or higher.

Implantation depth concentration and crystalline distortion level profiles has been calculated using Low Energy Approximation. The electronic stopping power is calculated using the accurate Ziegler semi-empirical expression at a single energy and then employing the Lindhard assumption that the stopping power scales as the square root of energy to speed up the calculation.

At large vacancies concentration, of the order of 10^{22} which corresponds to 5.6% crystal disorder, diamond undergo graphitisation. This places a limit on implantation, however the best optical properties of are found at 7%-15% of crystal disorder. Nitrogen implantation with concentrations of 100 to 1000 ppm corresponding to crystal disorder from 5% to 16% respectively.

Detailed optical analysis of the CVD diamonds will be presented during the talk. Comparison between as grown and nitrogen implanted diamonds will be discussed based on photoluminescence and Raman spectra study. In addition time resolved photoluminescence study of implanted diamonds will be used to assess concentration of nitrogen atoms and crystal disorder influence on optical emission dynamics.

Acknowledgements:

We acknowledge financial support from European Commission (H2020-MSCA-RISE-2016, D-SPA, project ID 734578) and Department of Agriculture, Food and the Marine, Ireland (project reference15/F/679).

Keywords: nitrogen implantation, optical properties, CVD bulk diamond, diamond films

Effect of graphene oxide additive on tribocorrosion behavior of MAO coatings prepared on Ti6Al4V alloy

You Zuo, Tianlu Li, Peihang Yu, Fei Chen

(Department of Materials Science and Engineering, Beijing Institute of Petrochemical Technology)
chenfei@bipt.edu.cn

Abstract: It is proved that titanium and its alloys possess the priority on corrosion resistance and the shortage on wear resistance. So tribocorrosion, a study orientation fascinating researchers from recent years and considering the both corrosion and wear behavior of material, have to be considered on the titanium, its alloys and its surface treated materials. In this study, MAO coated Ti6Al4V alloys with graphene oxide (GO) additive and without additive were prepared by micro-arc oxidation (MAO) method in silicate electrolyte. The coatings were characterized by X-ray diffraction (XRD), scanning electrode microscope (SEM), energy dispersive spectrometer (EDS) and Raman spectrometer. The corrosion resistance and tribocorrosion were tested by an electrochemical workstation and an electrochemical and friction tester. The result demonstrated that the addicting of GO improved corrosion resistance of coating in a slight range and the tribocorrosion behavior was ameliorated evidently.

Keywords: micro-arc oxidation, graphene oxide, Ti6Al4V alloy, corrosion resistance, tribocorrosion

Study on energy resolution of high quality single crystal diamond α particle detector

Yanzhao Guo, Jinlong Liu, Yun Zhao, Yuting Zheng, Liangxian Chen, Junjun Wei, Chengming Li
(Institute of Advanced Materials and Technology, University of Science and Technology Beijing)
chengmli@mater.ustb.edu.cn

Abstract: Chemical vapor deposition (CVD) diamond is being developed as radiation hard material for replacement or upgrade to present detectors in extreme radiation environments. However, its use in practical applications has been inhibited by space charge stability issues caused by nitrogen impurity concentrations within the material.

In this study, High quality CVD single crystal diamond (SCD) detectors with different concentrations of nitrogen impurities have been fabricated and characterized. The SCD substrates have been synthesized by microwave plasma assisted chemical vapor deposition (MPCVD) in a 6kw dome-type microwave reaction chamber. High quality free standing SCD films (3.5 mm \times 3.5 mm \times 0.4 mm) have been obtained after polishing and cutting from high-pressure, high-temperature (HPHT) seed substrate. The SCD samples have been characterized using several methods including Raman, stereomicroscope, laser confocal microscope, X-ray rocking curves, Infrared and UV-Vis-NIR absorption spectra, Electron paramagnetic resonance (EPR) and other traditional techniques. The membranes have been found to be of exceptional purity with respect to intrinsic and extrinsic defects, showing a different low nitrogen concentration. In addition, the optimal growth conditions and careful substrate preparation have resulted in a very low dislocation density. To determine the optimal electrode material, the energy lost has been calculated by stopping and range of ions in matter (SRIM) simulation of α particle in the metal layers of the electrode. The dark current and spectroscopic resolution under alpha particle irradiation have been investigated. Next, the effect of different nitrogen impurity concentrations on the diamond detector performance has been analyzed.

Keywords: single crystal diamond, nitrogen impurity, detector, α particle

Effect of micro-arc oxidation electrolyte and voltage on growth of LDHs film

Peihang Yu¹, Fei Chen², You Zuo¹, Tianlu Li², You Zhang²

(1. Beijing University of Chemical Technology; 2. Beijing Institute of Petrochemical Technology)
yupeihang@bipt.edu.cn

Abstract: Micro-arc oxidation (MAO) technology was used to prepare the ceramic layer on the surface of 2024 aluminum alloy, and LDHs film was in-situ grown on the surface of the ceramic layer by a chemical method to repair defects (micro-cracks and micro-pores) of MAO ceramic layer. Through the analysis of SEM, XRD and GDOES, it was found that LDHs film have been successfully grown on ceramic layer prepared in silicate electrolyte, but the film did not grow uniformly. This may be because the ceramic layer prepared from the silicate electrolyte contained Si element that suppress the nucleation and growth of LDHs crystal grains. Therefore, the effect of ceramic layers prepared from silicate electrolytes and meta-aluminate electrolytes on the growth of LDHs films was discussed. It was found that the ceramic layer prepared with meta-aluminates was more conducive to the growth of LDHs. At the same time, we also analyzed the effect of different ceramic layers prepared by different voltages on the growth of LDHs film under the constant current mode of micro-arc oxidation power supply.

Keywords: micro-arc oxidation, electrolyte, voltage, growth, 2024 aluminum alloy

Superhard nanocomposite films deposited by filtered cathodic vacuum arc

Xu Zhang, Bin Liao, Han Zhou, Minju Ying, Yongqing Shen, Xiangying Wu

(Key Laboratory of Beam Technology of Ministry of Education,
College of Nuclear Science and Technology, Beijing Normal University)
zhangxu@bnu.edu.cn

Abstract: Nanocomposite coatings composed of crystalline/amorphous nanophases mixture have recently attracted increasing interest with respect to fundamental research and industrial applications, because of the possibilities of synthesizing a surface protection layer with a combination of mechanical and tribological properties that are often not attained even in nanocrystalline materials, such as high hardness and toughness, superior wear resistance and low friction. The titanium carbide/amorphous carbon nanocomposite films were deposited on silicon substrate by filtered cathodic vacuum arc (FCVA) technology. The composition and structures of the titanium carbide/amorphous carbon nanocomposite films were studied by scan electronic spectroscopes, X-ray diffraction, Raman and X-ray photoelectron spectroscopes. The hardness and elastic modulus of the titanium carbide/amorphous carbon nanocomposite films were higher than 50 GPa and 400 GPa respectively determined by nano indentation tests. The nanocomposite nc-ZrCN/a-CN_x films with a carbon content varying from 34 to 61 at% were deposited under different C₂H₂/N₂ reactive gas flow. Results showed that nanocomposite nc-ZrCN/a-CN_x films were composed of about 8 nm sized ZrCN nanocrystalline embedded in different amount of a-CN_x amorphous matrix. Mechanical properties of nanocomposite nc-ZrCN/a-CN_x films showed a significant dependency on thickness of a-CN_x matrix. Nanocomposite nc-ZrCN/a-CN_x film reached the highest hardness (41 GPa) and reduced modulus (320 GPa) when the thickness of a-CN_x matrix was around 0.4 nm. Nanocomposite nc-ZrCN/a-CN_x film at higher carbon content has lower friction coefficient (0.2) and better wear resistance.

Keywords: superhard, filtered arc, nanocomposite film, microstructure

Ultra-smooth and hydrophobic ultra-nano-crystalline diamond film growth in C-H-O-N gas phase system via microwave plasma CVD

Yuting Zheng¹, Jinlong Liu¹, Zhina Qi¹, Haitao Ye², Fangsen Li³, Hui Hao³, Chengming Li¹

(1. Institute for Advanced Materials and Technology, University of Science and Technology Beijing;

2. School of Engineering and Applied Science, Aston University;

3. Suzhou Institute of Nano-Tech and Nano-Bionics(SINANO), Chinese Academy of Sciences)

chengmli@mater.ustb.edu.cn

Abstract: Surface hydrophobicity and smoothness of deposited diamond film are extremely significant factors for engineering application. In this study, ultra-smooth and hydrophobic nitrogen-incorporated ultra-nano-crystalline diamond (UNCD) film was synthesized by microwave plasma chemical vapour deposition (MPCVD) in CH₄/H₂/O₂/N₂ system. The gas phase chemistries, surface roughness, morphology, growth rate, film chemical composition, quality and surface wettability were examined. It was found that OH, CN and CH⁺ groups play an important role in smooth UNCD synthesis in the C-H-O-N system, and the addition of oxygen could improve the crystal quality and surface roughness of the film. The refined UNCD film could be deposited at a fast growth rate 1.21 μm/h under the coupled effect of the gas phases (nitrogen/oxygen addition ratio (NOAR) = 6) in the recess of molybdenum holder on polycrystalline diamond (PCD). Meanwhile, the grain size (down to less than 10 nm) is reduced with the increase of nitrogen addition from 1 to 3 sccm as well as surface roughness (down to RMS 1.29 nm). Under this condition, the contact angle between UNCD film and water could be achieved to 105.5°. However, surface roughness goes up inversely and spherical nano-crystalline cluster will turn to worm-like shape with the rising of nitrogen flow alone to 10 sccm.

Keywords: chemical vapour deposition, ultra-nano-crystalline diamond, surface roughness, spectroscopy, surface hydrophobicity

Structure and tribocorrosion properties of coupled coatings of

TiSiCN/nitride on Ti6Al4V alloy

Minpeng Dong, Jinlong Li, Yebiao Zhu, Chunting Wang, Fuliang Ma, Liping Wang

(Ningbo Institute of Material Technology and Engineering)

lijl@nimte.ac.cn

Abstract: In order to improve the poor wear resistance of Ti6Al4V alloy, the coupled coatings of TiSiCN/nitride were prepared by gas nitriding and arc ion plating. The structure, hardness and tribocorrosion behavior of the coating in seawater were studied. The structure and element chemical states were measured by SEM, XRD and XPS, respectively. The hardness was measured using Nano-Indenter G200. The tribocorrosion tests in artificial seawater were performed using a reciprocating ball-on-plate tribometer (Rtec) and a potentiostat (Modulab). The results show that the TiSiCN coating had distinct columnar structure and a same total thickness of about 2.45 μm. Moreover, the coupled coatings of TiSiCN/nitride exhibit maximum hardness of 36 GPa. Compared with Ti6Al4V substrate, the TiSiCN/nitride coupled coatings have a low corrosion current density, higher corrosion potential, low friction coefficient and excellent wear resistance in either ambient air or artificial sea water.

Keywords: coupled coatings of TiSiCN/nitride, gas nitriding, arc ion plating, structure, tribocorrosion properties

Excellent adhered thick diamond-like carbon coatings by optimizing hetero-interfaces with sequential highly energetic Cr and C ion treatment

Liangliang Liu, Zhongzhen Wu, Xiaokai An, Wei Tang
(Peking University Shenzhen Graduate School)
wuzz@pkusz.edu.cn

Abstract: Diamond-like carbon (DLC) coatings have attracted much attention due to their excellent hardness, low friction, and superior corrosion resistance. Unfortunately, the poor adhesion caused by internal stress limits the typical thickness to 3-5 μm . This paper presents a novel interlayer design and interface engineering and the induced excellent adhesion of thick diamond-like carbon (DLC) coatings on the high speed steel substrate. The interlayer has fundamentally a graded Cr/CrC_x/CrC/DLC structure, but various treatments to the hetero-interfaces have been conducted including sequential energetic ion bombardments with Cr at the substrate/Cr interface using high-power impulse magnetron sputtering (HiPIMS) and with C at the CrC/DLC interface using an anode layer ion source. It has been observed that the critical load has been improved from 18 N for a single Cr interlayer to 77 N for a Cr/CrC_x/CrC interlayer for thick DLC coatings of 13 μm . Using the same design, a very high critical load of 73 N has been achieved on the ultra-thick DLC coating of 50 μm . This interlayer design has allowed the deposition of a DLC coating that is not only thick but also hard with excellent tribological properties. The DLC coatings have a high hardness of >18 GPa, a low friction coefficient of 0.12 and a low wear rate of $(1.7\pm 0.2)\times 10^{-15}$ m³/N m. This paper discusses the effect of the ion bombardment of the interlayer on the coating adhesion and the strengthening mechanisms.

Keywords: thick DLC films, graded interlayer, energetic ion beam bombardment, adhesion

Element diffusion and self-healing performance of MoSiAlY coating on γ -TiAl substrate by a surface alloying method at 900 °C

Yi Xu^{1,2}, Pengfei Shi¹, Angjian Wu², Jie Qiu², Shiyu Cui³, Wanhui Liu¹, Ting Yuan¹,
Liwei Zhang¹, Qiang Miao³

- (1. Department of Chemistry and Materials Engineering, Changshu Institute of Technology, China;
 2. Department of Materials Science and Engineering, University of California at Berkeley, United States;
 3. College of Materials Science and Technology, Nanjing University of Aeronautics and Astronautics, China)
- xuyi@cslg.edu.cn

Abstract: A novel MoSiAlY coating was developed on γ -TiAl alloy by double glow plasma surface alloying technology. This study focused on the element diffusion behavior and self-healing performance of MoSiAlY coating at 900 °C oxidation test for 300 h. The results indicated that the oxidation resistance of γ -TiAl alloy was effectively improved by MoSiAlY coating. As the exposure time increasing, it is interesting that more and more cracks in the coating surface had been self-healed because of the formation of Mo₂O₃ and the element diffusion of Aluminium. The phase of coating surface mainly consisted of Mo₂O₃, Al₂O₃ and Y₂O₃ after oxidation test. The average mass gain of MoSiAlY coated samples was 3.71 mg/cm² under exposure at 900 °C for 300 h, comparing with 15.77 mg/cm² of substrate. This coating may be potential surface enhancement for Ti-Al intermetallics at high temperatures.

Keywords: element diffusion, self-healing performance, MoSiAlY coating

The behavior of Ag in TiSiN coating and the properties of the composite coating

Yebiao Zhu, Minpeng Dong, Jinlong Li, Keke Chang, Liping Wang
(Ningbo Institute of Materials Technology and Engineering, Chinese Academy of Sciences)
zhuyebiao@nimte.ac.cn

Abstract: Nowadays, a lot of moving parts in marine and aircraft engineering are worn out with their service time increasing. PVD coating are therefore needed for these parts and TiSiN is a kind of superhard coating whose hardness can reach to 105 GPa. However, TiSiN has a relatively high friction coefficient and seriously abraded. Besides, in marine engineering, seaweeds will grow on the coating and foul it until the substrate is exposed. So we need a multifunctional coating to adapt different environment. We added Ag element to the TiSiN coating. In this experiment, TiSiN and Ag layers were deposited alternately on Ti-6Al-4V using reactive co-sputtering in multi-arc ion plating system. The Ag atoms had a high diffusivity therefore they can diffuse from the middle of the coating to the surface. We use VASP and OPENMX based on DFT to calculate how the Ag diffuse in the TiSiN coating and the result is that the Ag atoms prefer to diffuse through the boundaries of TiN nanocrystal and amorphous Si₃N₄. Because of that, when coating was scratched and fabricate lots of boundaries, Ag atoms would diffuse to the wounds and heal them. In addition, The TiSiN coating maintained high hardness with Ag doped so the coating keep good mechanics property and the Ag atoms diffusing to the surface of coating endowed the coating with new properties such as anti-bacterial capability and friction-reducing property. So the composite coating can solve the problem of wearing and fouling.

Keywords: diffuse, self healing, anti-bacterial, lubrication

Tribological behavior of epoxy coatings modified by nano filler (Al₂O₃/WC-Co)

Yuqin Yan, Pingze Zhang, Dongbo Wei, Fengkun Li
(Materials Science and Technology, Nanjing University of Aeronautics and Astronautics, Nanjing, China)
qinyanyu@nuaa.edu.cn

Abstract: This study investigates the effects of adding nano filler (Al₂O₃/WC-Co) in the epoxy resin coating during dry sliding under ambient temperature. Al₂O₃ and WC-Co have exceptional hardness as ceramic particles, which is envisioned to enhance hardness of epoxy coating while maintaining toughness, thereby enhancing wear resistance. In this paper, Al₂O₃ and WC-Co reinforced epoxy resin coatings were successfully fabricated by air spraying process on the surface of TC18 alloy. The wear behaviours of the base alloy and coatings were comparatively studied. The addition of ceramic particles led to an enhancement of wear resistance of 64.7%-69% and 59.4%-62% in Epoxy/Al₂O₃ and Epoxy/WC-Co coatings respectively compared with that of the substrate. TC18 abases alloy mainly showed abrasive wear, while epoxy/Al₂O₃ and epoxy/WC-Co coatings showed adhesive wear. The resin in the coating will soften or even carbonized in the friction state, so as to play a role in lubrication, but a long time of reciprocating friction made the friction contact surface delamination

Keywords: epoxy/Al₂O₃ coating, epoxy/WC-Co coating, friction and wear, TC18 alloy

Study on the modification of high energy titanium ion implantation on the surface of aluminum alloy

Gaohui Zhang, Kecheng Chen, Fengming Li, Yang Wang
(Institute of Surface Physics, China Jiliang University)
ghzhanggh@163.com

Abstract: Aluminum alloy is a kind of nonferrous metal structural materials widely used in industry due to their low density, high strength and good plasticity. High energy titanium ion is implanted into the surface of aluminum alloy by high energy metal ion implantation (MEVVA source) to improve its surface strength and enhance its corrosion resistance under special environment. The XPS technique is used to test the surface composition after ion implantation, the morphology of the aluminum alloy surface after ion implantation is observed by atomic force microscopy, and the corrosion resistance of aluminum alloy under the chloride environment after ion implantation is measured in a 5% NaCl solution at room temperature. The results indicate that the surface morphology of aluminum alloy is basically unchanged after ion implantation, and there is titanium phase on the surface, with the increase of the amount of titanium ions implanted, the corrosion resistance is increased.

Keywords: aluminum alloy, ion implantation, corrosion resistance

Si-DLC films with excellent tribomechanical properties

Chaoqian Guo¹, Songsheng Lin¹, Qian Shi¹, Chunbei Wei¹, Hong Li², Yifan Su²
(1. Guangdong Institute of New Materials; 2. Anode Layer Ion Source)
cqguo12s@alum.imr.ac.cn

Abstract: Si-DLC films were deposited by anode layer ion source combined with high power pulsed magnetron sputtering on carbides and silicon wafers. Scanning electron microscope was used to observe surface morphology and cross-sectional morphology of films. Roughness of Si-DLC films was measured by surface profilometry. X-ray photoelectron spectroscopy and Raman spectrometer were used to analyse chemical bonding states in Si-DLC films. Hardnesses of the films were investigated by nano-indentor as well as elastic modulus. Critical loads between Si-DLC films and carbides substrates were obtained by scratch tester. Coefficients of friction were measured by a ball-on-disk tribometer. And wear rates of different Si-DLC films were calculated according to the formula $W=V/F \cdot L$. Si-DLC films displayed excellent wear resistance.

Keywords: Si-DLC, tribomechanical properties, anode layer ion source, HIPIMS

Abrasion and erosion behavior of DLC-coated oil-well tubing in a heavy oil / sand environment

Liangliang Liu, Zhongzhen Wu, Xiaokai An, Wei Tang
(Peking University Shenzhen Graduate School)
wuzz@pkusz.edu.cn

Abstract: The sucker rod pump, an important machine in oil exploration and extraction, normally works in a heavy oil / sand environment in which severe abrasion and erosion occur, especially on oil-well tubing. To improve the service life, DLC coatings with different thicknesses are fabricated on the oil-well tubing and the mechanical, tribological, and anti-corrosion properties are investigated. The results show that the thickness can be compromised with adhesion due to the low stress induced by alternate implantation and deposition at the pulsed high-voltage bias. Compared to severe abrasion of the carbonitriding AISI 1045 oilwell tubing, the thick DLC coatings have good anti-abrasion properties in the heavy oil / sand environment. Moreover, excellent erosion resistance properties is observed from the DLC-coated samples as exemplified by the small corrosion current density and high corrosion potential. The tests conducted in both simulated and practical working conditions reveal that the service life of the oil-well tubing is significantly improved.

Keywords: abrasion and corrosion, DLC coatings, thickness, heavy oil sand environment

Synthesis of monolayer MoN and nanomultilayer MoN/CrN coatings using cathode arc plasma vapor deposition

Canxin Tian, Zesong Wang
(Lingnan Normal University)
cxtian@lingnan.edu.cn

Abstract: Synthesis of monolayer MoN and nano-multilayer MoN/CrN coatings using cathode arc plasma vapor deposition was studied in this work. The coatings were characterized in terms of crystal phase, microstructure, surface morphology and mechanical properties by transmission electron microscopy (TEM), X-ray diffractometry (XRD), atomic force microscope (AFM) and microhardness tester. Results from TEM and XRD analysis showed that the crystal structure of MoN and MoN/CrN coatings has a cubic lattice structure. The modulation period of MoN/CrN coatings from 58.5 nm to 11.17 nm with increasing substrate rotation speed in the range of 1-10 rpm. The maximum hardness of MoN/CrN nanomultilayer coatings, when the rotation speed is 7 rpm and the modulation period 15 nm, are approximately 2950 HV. The value is 1.5 times higher than those of the MoN single layer coating (2000 HV). These enhancement effects in superlattice films could be attributed to the resistance to dislocation glide across interface between the MoN and CrN layers.

Keywords: MoN coatings, MoN/CrN coatings, modulation period, microhardness

Effect of cathode arc current on the oxidation and seawater corrosion resistance properties of Cr-Si-N coatings deposited by cathode rotating arc ion plating

Yanxiong Xiang, Canxin Tian, Feng Liang, Changwei Zou
(Lingnan Normal University)
zoucw@lingnan.edu.cn

Abstract: Superhard nanocomposite coatings, which were prepared by physical vapor deposition technology, played an important role in the surface modification of engineering components in various industrial environments owing to their properties such as high hardness, good tribological properties, oxidation resistance and corrosion resistance. Cr-Si-N coatings were fabricated by cathode rotating arc ion plating technique under varying deposition cathode arc current. The results showed that an amorphous/nanocrystalline structure containing CrN and Si₃N₄ phases was observed for Cr-Si-N coating. The hardness of the Cr-Si-N coatings deposited at 80 A CrSi target current are up to approximately 3200 HV200 and the friction coefficient is lower than 0.2. The high-temperature oxidation resistance behavior and corrosion resistance properties of the Cr-Si-N coatings were detailed studied using high temperature muffle furnace and electrochemical working station in 3.5% NaCl solution. The adhesion, internal stress and toughness of coating played the key role in improving the wear situation in seawater, which could effectively inhibit the generation and propagation of crack in the coatings. Meanwhile, the protective capability of coatings could be improved by proper cathode arc current, which could enhance the densification of coating. In addition, the Cr-Si-N coating under cathode current of 80 A presented the lowest friction coefficient of 0.12 and wear rate of $1.32 \times 10^{-7} \text{ mm}^3/(\text{N m})$ in seawater, indicating the best anti-friction and anti-wear abilities.

Keywords: superhard nanocomposite coatings, Cr-Si-N, oxidation resistance, seawater corrosion resistance, cathode rotating arc ion plating

Hard and highly adhered a-C:H gradient coating fabricated by stress editing

Xiaokai An, Zhongzhen Wu, Liangliang Liu, Wei Tang
(School of Advanced Materials, Peking University Shenzhen Graduate School, Shenzhen 518055, China)
wuzz@pkusz.edu.cn

Abstract: Diamond like carbon (a-C:H) coatings is famous for the low friction coefficient, however, notorious for the high residual stress. The hardness depending on the sp³ proportion increases not only the coating-life but also the residual stress, inducing easily peeling off especially for the thick coatings. This paper develops several thick a-C:H coatings (>10 μm) with different stress and hardness by various bias applications, respectively. Furthermore, a new stress editing method is used to decrease the stress accumulation however to keep the high hardness of the coatings. The results show that a low compressive residual stress of about 0.42-0.84 GPa is obtained on the a-C:H coatings with the thickness of more than 8 μm, resulting in very high critical load of 63-74 N, while the obtained hardness is over 26 GPa. Besides, excellent tribological properties and corrosion resistance with the smaller friction coefficient of 0.13, lower wear rate of $1.01 \times 10^{-15} \text{ m}^3/(\text{N m})$, higher corrosion potential of -479.6 mV and lower corrosion current density of $1.77 \mu\text{A}/\text{cm}^2$ are revealed.

Keywords: a-C:H, stress editing, high hardness, adhesion

Effects of Ta, W doping on O adsorption and oxidation at the γ TiAl (111) surface

Yuqin Yan, Pingze Zhang, Dongbo Wei, Fengkun Li

(Materials Science and Technology, Nanjing University of Aeronautics and Astronautics, Nanjing, China)
pzzhang@nuaa.edu.cn

Abstract: The oxygen adsorption energies of Ta and W before and after the doping on the clean γ TiAl (111) surface were calculated by using a first-principles plane-wave pseudopotential method, the effect of alloying on the relative stabilities of different O adsorption sites were also analyzed. The results showed that oxygen atoms are more easily adsorbed on the fccAl site on the γ -TiAl (111) surface. After doping Ta and W, the stable adsorption position of oxygen has changed obviously, from the previous fcc-Al to hcp-Ti and hcp-Al. The adsorption of oxygen on the surface of γ -TiAl based alloys is chemisorption, and covalent and ionic bonding exists between oxygen and surface Al and Ti. This makes TiAl intermetallic compounds produce TiO₂ and Al₂O₃ at the same time when they are oxidized. Doping Ta and W alloying elements can inhibit the oxidation of Ti in the inner layer, which is beneficial to reduce the formation of harmful oxide TiO₂. At the same time, Ta, W and Ti, Al will bond each other to form new intermetallic compounds, thus reducing the Ti-Al bond

Keywords: γ -TiAl, oxidation, adsorption energy, first principle

Surface functionalized diamond for advanced engineering application

Haitao Ye

(Department of Engineering, University of Leicester, Leicester, LE1 7RH, UK)
hy122@leicester.ac.uk

Abstract: Diamond thin films and coatings have been traditionally used in cutting tools for various applications in nonferrous metal processing as they have superior sharpness and excellent wear resistance. Diamond based powders have been commercially used for polishing industry in order to get a superb mirror finish or remove scratches and marks on glass, stone or hard metals. Besides these commercial applications based on diamond's outstanding mechanical properties, diamond is also an ultimate semiconducting material of promise due to its superior physical, chemical and electronic properties over conventional semiconductors. Diamond electronics is a potentially disruptive technology in the medium-to long-term with specific applications in high power, high temperature and high frequency devices. This talk reviews the present status and future prospects of thin film diamond growth and its advanced engineering applications. The application of nanodiamonds for cold water cleaning and antimicrobial resistance will also be discussed. His research work on 'Nanodiamond for Cold Water Cleaning' demonstrated for the first time that surface functionalised nanodiamonds could improve the efficiency of removal of lipids, highlighting the potential of this process to make global energy savings and domestic washing machines much more efficient; this work has opened up a new research direction on nanoparticles additives research.

Keywords: surface functionalized diamond, advanced engineering application

Analysis of residual stress and interface bonding strength of TiN coating

Lihuan Wang, Liangxiang Chen, Jinlong Liu, Junjun Wei, Chengming Li

(Institute of Advanced Materials and Technology, University of Science and Technology Beijing)

chengmli@mater.ustb.edu.cn

Abstract: In this paper, based on the Ti-based PVD coating, the optimization of the design of the bearing friction system of the hemispherical dynamic pressure motor is studied. For the differences between physical parameters of Be, Ti and TiN materials, Abaqus finite element numerical calculation method was used to simulate and analyze the singlelayer TiN coating on the surface of the Be material, increase the Ti transition layer, gradient coating and graded coating, and the stress distribution status of the coating substrate under different conditions. Then simulation of hemispherical model with DLC coating was added. The results show that the trend of residual thermal stress at the interface of the coatings is consistent when the coating structure is changed in the same manner in different models. Only increase the coating thickness, the interface stress increases. Under the same thickness coating condition, as the thickness of the transition layer increases, the residual thermal stress value decreases. Increasing the number of coatings does not effectively reduce residual thermal stress. When the transition layer gradually transitions from the physical parameters of Ti to TiN, the residual thermal stress at the interface of the coating substrate is the smallest. This result has guiding significance for the optimal design of hard coatings.

Keywords: residual stresses, hemispherical, coating, interface strength

Effect of programmable ion permeation (PIP) technology on microstructure and corrosion resistance of 304 stainless steel

Wenming Li¹, Defu Luo², Ruipeng Han², Zhihong Li¹

(1. Hunan Honyu Wear-Resistant New Materials Co., Ltd.;

2. College of Materials Science and Engineering, Xihua University)

609808323@qq.com

Abstract: In this paper, the "orthogonal test" method was used to study the main process parameters of PIP ion infiltration process: temperature, time and effective infiltration agent concentration on the microstructure and corrosion resistance of 304 stainless steel, and the optimal process parameters were obtained. The microstructure, phase composition, wear morphology and electrochemical polarization curves of the PIP treated modified layer were studied by metallographic microscope, X-ray diffractometer (XRD), scanning electron microscope (SEM), friction and wear tester and electrochemical workstation. The results show that supersaturated γ NC single phase is formed after treated by PIP optimization process in 304 stainless steel, no CrN phase is precipitated; PIP layer hardness reaches 994 HV0.025, and the wear mechanism changes from adhesive wear before PIP treatment to abrasive wear after PIP treatment, the wear resistance is significantly improved. After PIP treatment, the corrosion potential E_{corr} increases from -0.183 mV to -0.162 mV, and the breakdown voltage E_p increases from -0.25 mV to 0.10 mV. The above results indicate that the single γ NC phase formed by PIP treatment can not only improve the wear resistance of stainless steel surface but also increase the pitting resistance of stainless steel.

Keywords: programmable ion permeation, 304 stainless steel, wear resistance, corrosion resistance

Plasma diagnostics in HiPIMS

Mike Hopkins
(Impedans Ltd.)
ailantech@163.com

Abstract: In high power impulse magnetron sputtering (HiPIMS), very high instantaneous power densities to the magnetron are used, which result in a dramatic increase of charge carriers in front of the target during the discharge pulse. For the HiPIMS discharge the electron density in the ionization region close to the target surface is on the order of 10^{18} - 10^{19} m⁻³[1,2]. For an electron density around 10^{19} m⁻³ the ionization mean free path of a sputtered metal atom is about 1 cm, while for an electron density of 10^{17} m⁻³, commonly observed in a direct current magnetron sputtering (DCMS) discharge, the ionization mean free path is approximately 50 cm for typical discharge conditions^[3]. Thus, given the high electron density in the HiPIMS discharge a significant fraction of the sputtered material is thereby ionized, which also has been verified in a great number of publications^[4-7].

An important parameter to understand is the ratio of ion to neutral deposition rates which gives insight into the ionized flux fraction. A retarding field analyzer with integrate quartz crystal microbalance design will be presented. This device can be configured to turn on and off the flow of ions to the crystal, thus enabling a measurement of the deposition rate due to ions compared to that due to neutral species. Sample data from various process applications will be presented along with comparisons against other diagnostic techniques.

Also, some results of a deposition tolerant Langmuir probe will also be presented. This probe continues to work when insulating layers are deposited on it. The probe can be synchronised with the HiPIMS pulse to time resolve the data capture through the pulse period. Results from a HiPIMS application will also be presented.

Keywords: HiPIMS, magnetron

Reference:

- [1] J.T. Gudmundsson, P. Sigurjonsson, P. Larsson, D. Lundin, and U. Helmersson, *J. Appl. Phys.* 105, 123302 (2009).
- [2] J. Bohlmark, J.T. Gudmundsson, J. Alami, M. Lattemann, and U. Helmersson, *IEEE Trans. Plasma Sci.* 33, 346 (2005).
- [3] J.T. Gudmundsson, *Vacuum* 84, 1360 (2010).
- [4] V. Kouznetsov, K. Mac ák, J.M. Schneider, U. Helmersson, and I. Petrov, *Surf. Coat. Technol.* 122, 290 (1999).
- [5] J. Vlcek, P. Kudlacek, K. Burcalova, and J. Musil, *Europhys. Lett.* 77, 45002 (2007).
- [6] J. Bohlmark, J. Alami, C. Christou, A.P. Ehiasarian, and U. Helmersson, *J. Vac. Sci. Technol. A* 23, 18 (2005).
- [7] K. Mac ák, V. Kouznetsov, J. Schneider, U. Helmersson, and I. Petrov, *J. Vac. Sci. Technol. A* 18, 1533 (2000).